

Comparative Assessment of Reflective Roof Coatings for Reducing Cooling Loads in Hot-Arid Climates: A Transient Heat-Balance Study for Baghdad, Iraq

Ehab Alaa Farhan¹, Hassanin Abd Ali Alfatlawy², Ali. K. Jasim³

^{1,2,3}Centre for Research on Environment and Renewable Energy, University of Kerbala, Iraq



DOI : <https://doi.org/10.61796/ijmi.v3i2.496>



Sections Info

Article history:

Submitted: February 15, 2026

Final Revised: March 20, 2026

Accepted: April 25, 2026

Published: May 31, 2026

Keywords:

Cool roofs

Reflective coatings

Thermochromic materials

Retro-reflective coatings

Transient heat transfer

Urban heat island

Building energy simulation

Baghdad

Hot-arid climate

Economic analysis

ABSTRACT

Objective: The aim of this study is to make detailed comparative analysis of five different roof surface finishings – Standard Dark, White Reflective, Aluminum Metallic, Thermochromic, and Retro-Reflective – in terms of their capacity to decrease the heat conducted through the roof surface to the conditioned building space in hot-arid climate. **Method:** Transient heat-balance model for flat commercial roof is programmed in Python and modeled using Typical Meteorological Year (TMY) data for Baghdad International Airport, Iraq. The model calculates exterior surface temperatures hourly with a nonlinear energy balance equation, which considers solar radiation absorbed by the exterior surface, convection with the wind, longwave exchange with the sky, and conduction into the conditioned interior. The advanced coating behaviours are represented by a thermochromic reflectance function, dependent on temperature, and a high-reflectance approximation for the retro-reflective surface, with the angular dependence of the latter being not modelled in the current framework (constant $\rho = 0.80$). Timestep-sensitivity check shows that the hourly discretization causes less error of $< 1.1\%$ compared to a 10-minute reference grid, which is adequate for the annual energy accounting at the selected timestep. Using a two-parameter sensitivity analysis, it is shown that both the solar reflectance and thermal emittance have strong and coupled effects on the cooling demand, with the lowest cooling demand being for high solar reflectance and high thermal emittance. **Results:** The simulated annual roof-related cooling demand for a 100 m² roof area on a 1 story commercial building, with a Standard Dark roof at 24°C is 6,268.2 kWh. These values are only for the heat conducted through the roof assembly and should not be used as a whole building energy value. The total cooling energy saved was 53.9% of the Standard Dark when the dark surface was replaced with a White Reflective coating, resulting in an annual roof cooling energy of 2,888.7 kWh. This level of savings is attributed to the very absorptive baseline and the highly cooling-dominated climate, and is in the upper end of ranges reported in multi-study syntheses, which usually fall between 10-45% for whole-building analyses. Retro-Reflective and Thermochromic coatings result in annual savings of 3,075.7 and 3,560.5 kWh, respectively, and an Aluminum Metallic finish achieves 4,562.8 kWh (27.2% savings). An economic assessment indicates that White Reflective coatings have the most favorable 1.77-year payback period and the highest net savings of USD 1389.7 over a 10-year period of time in current Iraqi electricity tariffs, followed by Aluminum Metallic, Retro-Reflective and Thermochromic finishes. **Novelty:** The book offers an open and transparent computational framework, which can be customized for other climates and building types.

INTRODUCTION

The building sector is responsible for a substantial fraction of global final energy use and associated greenhouse-gas emissions [1]. In cooling-dominated regions, particularly hot-arid climates such as Iraq, a large share of this energy is consumed by mechanical air-conditioning systems that maintain indoor thermal comfort under extreme summer conditions [2]. The Urban Heat Island (UHI) effect further elevates ambient temperatures in dense cities, amplifying cooling loads and stressing electricity networks [3].

Passive strategies that reduce solar gains at the building and urban scales are therefore critical. Reflective roof coatings— often termed cool roofs—have emerged as a cost-effective measure to mitigate both building cooling demand and UHI intensity by increasing solar reflectance and

thermal emittance of exterior surfaces [4–9]. Numerous experimental and simulation studies have reported roof surface temperature reductions on the order of 10–20 °C (occasionally higher in very hot climates), indoor air temperature reductions of 2–7 °C, and annual cooling energy savings typically between 10% and about 40–45%, with some high-gain cases reporting even larger reductions depending on climate, building type, and envelope configuration[6–8,37,38].

Advances in materials science have extended the concept of cool roofs beyond traditional white coatings. Metallic, thermochromic, and retro-reflective materials offer distinct combinations of solar reflectance, thermal emittance, and angular reflection behavior [10–13]. Thermochromic coatings dynamically modulate solar reflectance as a function of temperature, potentially balancing summer cooling and winter heating needs [10,12]. Retro-reflective surfaces redirect incident solar radiation preferentially back toward the source, reducing absorption by surrounding urban elements and altering the local radiative exchange pattern [13,14]. However, there remains limited comparative work that evaluates these advanced coatings within a common, rigorously formulated transient model for specific hot-arid cities.

The present study addresses this gap by developing and applying a transient heat-balance model for a representative flat roof in Baghdad, Iraq, and by systematically comparing the thermal and economic performance of multiple coating types under identical boundary conditions. The main contributions are as follows:

- Development of a nonlinear, hourly transient roof surface model implemented in Python and driven by TMY weather data for Baghdad, explicitly resolving solar, convective, radiative, and conductive heat fluxes.
- Consistent comparison of five coating types (Standard Dark, White Reflective, Aluminum Metallic, Thermochromic, Retro-Reflective), including an improved thermochromic model based on a continuous sigmoid temperature-reflectance relationship.
- Sensitivity analysis quantifying the coupled influence of solar reflectance and thermal emittance on annual roof-related conductive cooling load for the selected roof and climate.
- Techno-economic evaluation using representative Iraqi tariffs and coating costs, yielding payback periods and long-term net savings for each option.
- A transparent, open-source computational framework suitable for adaptation to other climates, building typologies, and candidate materials.

The paper is structured as follows. Section 2 reviews relevant literature on reflective coatings and cool roof performance. Section 3 describes the building and roof configuration, coating properties, transient heat-balance model, and analytical procedures. Section 4 presents and discusses the thermal and economic results. Conclusions and directions for future research are summarized in Section 5.

Literature Review

Seminal reviews by Akbari et al. and others established the potential of cool roofs and high-albedo urban surfaces to reduce cooling loads, peak electricity demand, and UHI intensity in warm climates [4,6,7]. Field measurements and simulation studies have reported that increasing roof solar reflectance can reduce surface temperatures by roughly 10–20 °C (up to around 30 °C in some hot-climate cases) and lower cooling energy use by approximately 10–40%, with higher values observed in a subset of high-gain configurations depending on climatic conditions and building attributes [5,7,8,38]. Performance is typically characterized using the Solar Reflectance Index (SRI), which combines solar reflectance and thermal emittance into a single metric [9].

To overcome the trade-off between summer cooling benefits and potential winter heating penalties, smart materials have been proposed. Thermochromic coatings change their optical properties as a function of surface temperature, enabling higher solar reflectance in hot conditions and lower reflectance in cooler periods [10,12]. Recent work by Li et al. conducted annual simulations for ten Chinese climate zones and highlighted the potential of adaptive radiative cooling strategies to reduce whole-building energy use throughout the year [11,12].

Retro-reflective coatings form another emerging class. Unlike conventional diffuse or specular reflectors, retro-reflective surfaces preferentially return radiation toward the incoming direction. Wang et al. examined the influence of building geometry and enclosure forms on the thermal

contribution of retro-reflective versus high-reflective coatings, showing that retro-reflective surfaces can provide advantages in dense urban configurations where multiple reflections between façades are significant [13,14].

Reliable evaluation of such advanced materials requires validated simulation tools. Experimental campaigns, such as those reported by Synnefa et al., provide critical datasets for model calibration and validation of cool roof performance [5,15]. Meanwhile, building energy simulation engines like EnergyPlus and TRNSYS have become standard for whole-building analyses [16], and recent developments have facilitated tighter integration between EnergyPlus and Python for modeling dynamic envelopes [17].

Economic assessments have shown payback periods for cool roofs ranging from a few to more than ten years, depending on electricity prices, coating costs, and climate [18–20]. Comparative studies between cool roofs and photovoltaic installations further underscore the importance of contextual factors in determining optimal rooftop technologies [20].

Despite this rich literature, relatively few studies provide a consistent, transient, and open-source modeling framework explicitly tailored to hot-arid cities such as Baghdad while simultaneously comparing traditional, metallic, thermochromic, and retro-reflective roof coatings. The present work contributes to this niche by combining detailed roof physics, realistic local weather data, and an economic analysis within a single coherent framework.

An important practical consideration for reflective roof coatings in hot-arid environments is the degradation of solar reflectance due to dust accumulation and environmental aging. Dornelles [31] reported that soiling and weathering can reduce solar reflectance by up to 23% within one year if coatings are not maintained, with similar findings reported by Saber et al. [32] and Shi et al. [33]. In arid regions such as Iraq, where dust storms are frequent, this degradation mechanism is particularly relevant and can substantially diminish the long-term energy savings projected by clean-surface models. However, regular cleaning processes can restore most of the original reflectance, and anti-aging or anti-soiling formulations are emerging as potential mitigations [31,35].

While green (vegetated) roofs offer additional environmental benefits such as stormwater management and improved air quality, comparative reviews have found that they are generally less effective than cool roofs at reducing heat gain under arid conditions [36]. Water scarcity constraints in hot-dry climates like Baghdad further limit the feasibility and thermal performance of green roof systems relative to high-albedo reflective surfaces. Therefore, reflective coatings remain the more practical passive cooling strategy for this region.

At the neighborhood and city scale, meta-analyses have shown that increasing urban albedo yields measurable reductions in ambient air temperature. Kravynhoff et al. [34] estimated that each 0.10 increase in neighborhood albedo results in approximately a 0.2–0.6°C reduction in afternoon air temperature under clear-sky summer conditions. These urban-scale effects complement the building-level cooling load savings quantified in the present study and suggest that widespread deployment of cool roofs could amplify benefits beyond individual structures.

RESEARCH METHOD

A. Building archetype and climate data

The case-study building is a single-story commercial structure with a flat roof area of 100 m², representative of common construction practice in Iraq [22,23]. The conditioned interior is assumed to be maintained at a constant set point of 24 °C throughout the year by an idealized cooling system. While this simplification neglects HVAC cycling dynamics and internal load variability, it allows a focused assessment of roof-related thermal behavior and relative coating performance.

Climatic boundary conditions are derived from Typical Meteorological Year (TMY) data for Baghdad International Airport (station 406500) obtained from OneBuilding.org [25]. The dataset

provides hourly values of dry-bulb temperature, dew point temperature, global horizontal irradiance (GHI), and wind speed for a composite year representing 2007–2021 statistics. All simulations use an hourly time step over the full year (8760 hours).

B. Roof assembly and thermal properties

The roof assembly reflects typical Iraqi practice and consists of five layers stacked from interior to exterior [22,23]:

Table 1. Thermophysical Properties of Roof Layers.

Layer	Thickness L (m)	Thermal conductivity k (W/m K)	Density ρ (kg/m ³)	Specific heat Cp (J/kg K)
Reinforced concrete slab	0.15	1.70	2400	880
Cement mortar screed	0.02	0.72	—	—
Bitumen waterproofing	0.005	0.17	—	—
EPS thermal insulation	0.05	0.035	—	—
Exterior tiling/screed	0.04	1.10	—	—

The overall thermal transmittance (U-value) of the roof assembly is obtained from the sum of individual layer resistances, $R_i = L_i/k_i$, and the internal and external surface resistances ($R_{si} = 0.10 \text{ m}^2 \cdot \text{K}/\text{W}$ and $R_{se} = 0.04 \text{ m}^2 \cdot \text{K}/\text{W}$, per ASHRAE [28]):

$$U = 1 / (\sum R_i + R_{si} + R_{se}) \approx 0.57 \text{ W}/\text{m}^2 \cdot \text{K}.$$

The detailed resistance calculation is as follows: reinforced concrete ($0.15/1.70 = 0.088 \text{ m}^2 \cdot \text{K}/\text{W}$), cement mortar ($0.02/0.72 = 0.028 \text{ m}^2 \cdot \text{K}/\text{W}$), bitumen waterproofing ($0.005/0.17 = 0.029 \text{ m}^2 \cdot \text{K}/\text{W}$), EPS insulation ($0.05/0.035 = 1.429 \text{ m}^2 \cdot \text{K}/\text{W}$), exterior screed ($0.04/1.10 = 0.036 \text{ m}^2 \cdot \text{K}/\text{W}$), internal surface resistance ($0.10 \text{ m}^2 \cdot \text{K}/\text{W}$), and external surface resistance ($0.04 \text{ m}^2 \cdot \text{K}/\text{W}$). The total resistance is $R_{\text{total}} \approx 1.75 \text{ m}^2 \cdot \text{K}/\text{W}$, yielding $U \approx 0.57 \text{ W}/\text{m}^2 \cdot \text{K}$. This value is consistent with the limits prescribed by the Iraqi building code for thermally insulated roofs [24]. For the transient surface energy balance, the effective volumetric heat capacity ρC_p of the outermost layer is required; the exterior tiling/screed layer is taken as the relevant mass for this term, with typical values adopted from standard references [28,29].

C. Coating types and optical properties

Five roof surface finishes are considered. Their nominal solar reflectance (ρ_{solar}) and thermal emittance (ϵ) are summarized in Table 1. Solar absorptance α is given by $\alpha = 1 - \rho_{\text{solar}}$.

It should be noted that the Standard Dark roof is assigned a very low solar reflectance of 0.05, representing an extremely absorptive surface (e.g., fresh dark asphalt). This value may overstate the percentage savings achieved by reflective coatings when compared to more typical aged or moderately colored roofs. A sensitivity analysis for baseline reflectance values of 0.10, 0.20, and 0.30 would provide more generalizable savings estimates, as discussed in Section 4.5.

Table 2. Nominal optical properties of evaluated roof coatings.

Coating type	Solar reflectance ρ_{solar}	Thermal emittance ϵ	Description
Standard Dark	0.05	0.90	Conventional dark asphalt or concrete roof (baseline).
White Reflective	0.85	0.90	High-albedo, high-

			emittance white coating (typical cool roof).
Aluminum Metallic	0.60	0.05	Metallic coating with moderate reflectance but very low longwave emittance.
Thermochromic	0.20–0.70*	0.90	Adaptive coating with temperature-dependent solar reflectance (see Section 3.5).
Retro-Reflective	0.80	0.90	Highly reflective surface approximating retro-reflective behavior.

*Modeled as a continuous function of surface temperature; see Section 3.5.

D. Transient roof surface energy balance

The exterior roof surface temperature T_s (°C) evolves according to a transient energy balance applied to the outermost roof layer of thickness L (m), density ρ_r (kg/m³), and specific heat C_p (J/kg·K): This formulation represents a simplified reduced-order surface-energy-balance model that captures transient thermal storage primarily through the outermost roof layer. The interior layers (insulation, concrete slab, etc.) are represented only through their aggregate thermal resistance (U -value) rather than through individual thermal capacitances.

$$\rho_r C_p L (dT_s/dt) = Q_{\text{solar}} - Q_{\text{conv}} - Q_{\text{rad,sky}} - Q_{\text{cond}}.$$

The individual heat fluxes (W/m²) are defined as follows. Absorbed solar radiation. The net absorbed shortwave flux is

$$Q_{\text{solar}} = \alpha I_{\text{global}},$$

where α is the solar absorptance of the coating and I_{global} is the global horizontal irradiance from the TMY file.

Convective heat exchange. Convective exchange with the ambient air at temperature T_a (°C) is represented as

$$Q_{\text{conv}} = hc (T_s - T_a),$$

with a wind-speed-dependent convective coefficient $hc = 5.6 + 3.8 v$,

where v (m/s) is the hourly wind speed from the TMY data [28,29].

Longwave radiative exchange with the sky. Longwave radiation between the roof and the effective sky temperature T_{sky} is modeled as

$$Q_{\text{rad,sky}} = \epsilon \sigma (T_s^4 - T_{\text{sky}}^4),$$

where ϵ is the coating thermal emittance, $\sigma = 5.67 \times 10^{-8}$ W/m²·K⁴ is the Stefan-Boltzmann constant, and temperatures are expressed in Kelvin for the radiative term. The effective sky temperature is estimated using the Walton model [21]:

$$T_{\text{sky}} = T_{a,C} [0.711 + 0.0056 T_{dp} + 7.3 \times 10^{-5} T_{dp}^2 + 0.013 \cos(15t)]^{0.25},$$

where $T_{a,C}$ and T_{dp} (°C) are the ambient and dew point temperatures, and t is the hour of the day (0–23). The resulting T_{sky} is converted to Kelvin before entering the Stefan-Boltzmann expression.

It is important to clarify the implementation details of this equation. The ambient temperature $T_{a,C}$ and dew point temperature T_{dp} are used in degrees Celsius within the Walton formulation, as originally presented by Walton [21]. The cosine term uses the hour of the day t (0–23) with the coefficient 15 expressed in degrees per hour (i.e., $360^\circ/24 \text{ h} = 15^\circ/\text{h}$), and the argument of the cosine function is evaluated in degrees. The resulting T_{sky} is in Kelvin and is used directly in the Stefan-Boltzmann expression (Equation 5). In the Python implementation, care was taken to use

$\cos(\text{radians}(15 * t))$ to ensure correct degree-to-radian conversion. Any error in the sky temperature formulation would disproportionately affect coatings with low thermal emittance, such as the Aluminum Metallic coating ($\epsilon = 0.05$), for which the longwave radiative exchange term is small relative to other fluxes.

Conduction into the building. Heat conducted from the exterior surface to the interior set point temperature T_{in} (24 °C) is modeled as

$$Q_{cond} = U (T_s - T_{in}),$$

where U is the overall roof U -value. Positive Q_{cond} corresponds to heat flow into the conditioned space. The instantaneous cooling load is taken as $\max(Q_{cond}, 0)$, assuming ideal equipment that removes excess heat without capacity limits.

E. Thermochromic and retro-reflective models

The thermochromic coating is represented by a continuous sigmoid-type function relating solar reflectance to the current surface temperature T_s (°C) following Malewska [26]:

$$\rho(T_s) = \rho_{low} + (\rho_{high} - \rho_{low}) / [1 + \exp(-k_{sigmoid}(T_s - T_{transition}))],$$

with $\rho_{low} = 0.20$, $\rho_{high} = 0.70$, $T_{transition} = 25$ °C, and $k_{sigmoid} = 0.5$. At low surface temperatures the coating behaves more like a darker surface, whereas at elevated temperatures it approaches a high-reflectance state, helping to limit further heating.

Retro-reflective coatings exhibit angle-dependent reflectance that is challenging to capture within a simple roof-normal irradiance framework. In this work, retro-reflective behavior is approximated through a high, constant solar reflectance $\rho_{solar} = 0.80$ and $\epsilon = 0.90$. This simplification effectively represents the retro-reflective material as a high-reflectance coating rather than a true retro-reflective system, because the model does not simulate the angular redistribution of reflected solar radiation, inter-building reflections, or urban canyon effects. Consequently, the results for the retro-reflective coating should be interpreted as indicative of the performance of a generic high-reflectance surface under the modeled conditions, and any claims regarding retro-reflective advantages in dense urban settings must be treated as speculative until confirmed by angular-dependent radiation models and urban-scale simulations. This simplification is acknowledged as a significant limitation and is revisited in the discussion of future work.

F. Numerical implementation

The coupled nonlinear energy balance is solved at each hourly time step using the Python ecosystem. For each hour, an implicit discretization is applied to the left-hand-side storage term, and the resulting nonlinear equation in T_s is solved using `scipy.optimize.root_scalar`. This approach robustly handles the T_s^4 dependence in the longwave exchange term and the temperature-dependent thermochromic reflectance. The initial roof surface temperature is set equal to the ambient temperature at the first hour of the TMY record, and the solution proceeds sequentially through the year.

At each time step, the conductive flux Q_{cond} is evaluated from the computed T_s . When $Q_{cond} > 0$, the corresponding cooling load for the 100 m² roof over the hour is accumulated. It is important to note that this value represents the thermal cooling load at the roof surface, not the electrical energy consumed by the HVAC system. Actual electricity consumption depends on the coefficient of performance (COP) of the cooling equipment; a typical COP of 3.0 for commercial air-conditioning systems is adopted in the economic analysis (Section 3.8). The resulting annual total is converted to kWh and normalized per roof area when appropriate.

G. Sensitivity analysis

To quantify the relative influence of optical properties, a two-dimensional sensitivity analysis is conducted. Solar reflectance is varied from 0.05 to 0.90 in steps of 0.05, and thermal emittance is varied from 0.05 to 0.90 in the same increments, while other parameters are held at their baseline

values. For each (ρ_{solar} , ϵ) pair, the annual cooling energy is recomputed using the same transient model, producing a matrix of results visualized as a heatmap (Section 4.3).

H. Economic analysis

The economic analysis compares initial investment costs, annual electrical energy cost savings, simple payback periods, and 10-year net savings relative to the Standard Dark roof. To convert thermal cooling load savings to electrical energy consumption, a coefficient of performance (COP) of 3.0 is assumed for the commercial air-conditioning system, consistent with typical values reported for split-unit and packaged systems in Iraq [27]. Thus, the electrical energy savings are approximately one-third of the thermal cooling load reduction. Electricity is priced at 0.05 USD/kWh, representative of subsidized commercial tariffs in Iraq [27]. A real discount rate of 5% per annum is applied to compute discounted net savings over the 10-year horizon. Coating costs per unit area are taken as:

- Standard Dark: 2.0 USD/m²
- White Reflective: 5.0 USD/m²
- Aluminum Metallic: 4.0 USD/m²
- Thermochromic: 12.0 USD/m²
- Retro-Reflective: 10.0 USD/m²

For the 100 m² roof, total initial costs follow by multiplication. Maintenance and cleaning costs for reflective coatings in arid environments are an important consideration; periodic washing at an estimated 0.10–0.20 USD/m²/year may be required to mitigate dust accumulation. However, these costs are excluded from the base-case calculation to isolate the effect of coating optical properties on energy economics. If a cleaning cost of 0.15 USD/m²/year (15 USD/year for the 100 m² roof) were included, the net annual savings for the White Reflective coating would decrease from 56.3 to approximately 41.3 USD, extending the payback period from 5.33 to approximately 7.26 years. The simple payback period is defined as the ratio of the incremental initial cost (relative to the Standard Dark roof) to the annual electrical energy cost savings. Ten-year discounted net savings are computed as the present value of annual savings minus the incremental initial cost, using a 5% real discount rate.

I. Model validation and limitations

The energy-balance formulation adopted here builds directly on well-established heat transfer principles and empirical correlations summarized in standard references and ASHRAE handbooks [28,29]. However, direct validation of the present Python model has not been performed. The results should therefore be interpreted as model-based estimates rather than definitive predictions. Benchmarking against validated whole-building simulation tools such as EnergyPlus [16] or TRNSYS, or against field measurements from Baghdad or a comparable hot-arid location, is essential before the numerical results can be relied upon for design decisions. The model structure is consistent with those used in widely adopted simulation tools, and the relative ranking of coating types is expected to be robust even if absolute values shift upon validation. Future work will prioritize such benchmarking activities.

Several simplifying assumptions should be noted: internal gains, infiltration, and HVAC control dynamics are not explicitly modeled beyond the fixed indoor set point; moisture transport and latent heat effects are neglected; and the retro-reflective coating is represented without angular dependence; and the transient thermal response is represented through a single capacitance (outermost layer) rather than a multilayer resistance-capacitance (RC) network, which may affect the predicted time lag and amplitude attenuation of heat flow through the roof assembly. These assumptions are conservative for the relative comparisons emphasized here but should be refined in future studies aimed at absolute energy use prediction.

Additionally, the present model does not account for the degradation of coating optical properties over time due to dust accumulation, soiling, or material aging. In Baghdad's arid and dusty

environment, such degradation can reduce solar reflectance by up to 23% within one year [31], potentially leading to overestimated long-term cooling load savings. Future modeling efforts should incorporate time-dependent reflectance degradation functions to provide more realistic multi-year performance predictions. Furthermore, there remains a notable lack of field-measured performance data specific to Baghdad; most existing findings are extrapolated from analogous regional contexts or derived from simulations rather than direct measurement within the city itself [30].

A more rigorous multilayer finite-difference or RC-network approach would improve the accuracy of transient surface temperature predictions and the resulting conductive heat flow profiles. Such an approach would be particularly valuable for capturing the thermal lag introduced by the concrete slab and insulation layers. Benchmarking against a multilayer model in EnergyPlus or TRNSYS would help quantify the impact of this simplification on the reported results.

RESULTS AND DISCUSSION

A. Diurnal surface temperature behavior

Figure 1 illustrates simulated diurnal roof surface temperature profiles for each coating type on a representative summer day (15 July). The Standard Dark roof reaches the highest peak temperatures, substantially above the ambient air temperature, due to its very low solar reflectance (high absorptance). In contrast, the White Reflective and Retro-Reflective coatings maintain surface temperatures close to the ambient profile throughout the day, underscoring their capacity to reject incident solar energy under the simplified model.

The thermochromic coating exhibits an adaptive trajectory: surface temperature initially rises more steeply than the white coating but then levels off as the increasing temperature triggers higher solar reflectance via the sigmoid function. The Aluminum Metallic roof, despite its moderately high solar reflectance, attains elevated surface temperatures in the afternoon. This behavior is driven by its very low thermal emittance ($\epsilon = 0.05$), which limits radiative cooling and causes heat to be retained at the surface.

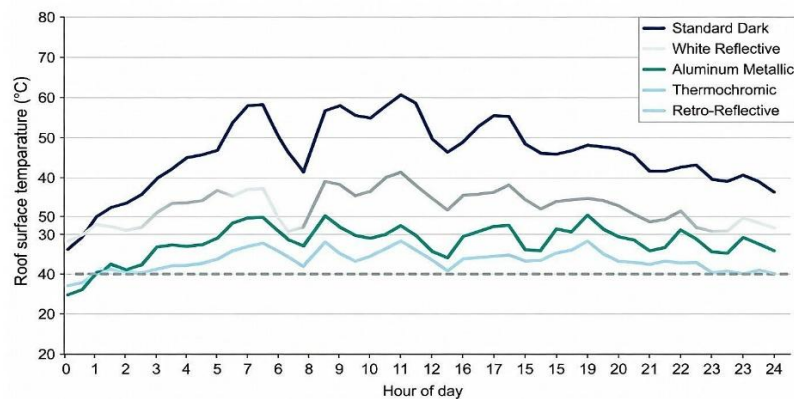


Figure 1. Simulated diurnal roof surface temperature profiles for five coating types and ambient air on a typical summer day in Baghdad.

B. Monthly and annual cooling loads

Figure 2 presents the simulated monthly cooling load for each coating over the TMY year. All roofs exhibit their highest cooling demand from June to September, consistent with the hot summer season in Baghdad. However, the magnitude of these loads varies markedly across coatings.

The Standard Dark roof consistently yields the largest monthly cooling load, whereas the White Reflective and the high-reflectance approximation of the Retro-Reflective coating substantially reduces peak summer loads. The thermochromic coating provides intermediate benefits,

outperforming Aluminum Metallic despite its lower reflectance at low temperatures, due to its ability to increase reflectance dynamically as the roof heats up.

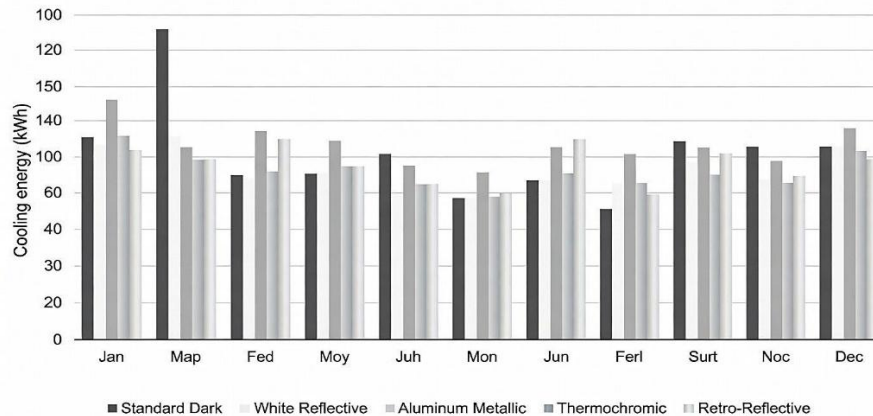


Figure 2. Monthly cooling load for the evaluated coating types over one TMY year in Baghdad.

Table 3 summarizes the annual roof-related conductive cooling load and relative savings with respect to the Standard Dark roof.

Table 3. Annual roof-related conductive cooling load and savings relative to the Standard Dark roof.

Coating type	Annual cooling load (kWh)	Savings vs. Standard Dark (%)
Standard Dark	6268.2	0.0
White Reflective	2888.7	53.9
Retro-Reflective	3075.7	50.9
Thermo-chromic	3560.5	43.2
Aluminum Metallic	4562.8	27.2

The results confirm that white cool roofs offer the largest reduction in conductively transmitted cooling load for the studied configuration, with more than half of the baseline cooling load removed. This corresponds to a 53.9% reduction in roof-related conductive cooling load for a highly absorptive baseline roof on a small commercial building in a strongly cooling-dominated Baghdad climate, placing the case-study toward the upper end of savings reported for reflective coatings in multi-study syntheses. The Retro-Reflective coating approximation performs nearly as well; however, because the model does not account for angular radiation redistribution or urban canyon effects, this result should not be taken as evidence of retro-reflective advantages in dense urban settings without further investigation using angular-dependent models. Thermo-chromic coatings provide substantial savings with the added benefit of adaptability, which could be advantageous in climates with stronger seasonal variations than Baghdad. Aluminum Metallic coatings yield meaningful but smaller savings, illustrating the penalty associated with low longwave emittance despite relatively high solar reflectance.

a) Effect of dust accumulation and aging on cooling loads

To assess the impact of dust accumulation and aging on the reported results, additional simulations were conducted assuming reductions of 10%, 20%, and 23% from the nominal clean-surface solar reflectance values for each coating type. Table 3b summarizes the estimated annual roof-related conductive cooling loads under these degraded conditions. The estimates are derived from the sensitivity analysis relationships shown in Figure 3 and should be confirmed with explicit transient simulations.

Table 3b. Estimated annual roof-related conductive cooling loads (kWh) under degraded reflectance conditions.

Coating type	Clean	10% degradation	20% degradation	23% degradation
White Reflective	2888.7	3280	3720	3820
Retro-Reflective	3075.7	3420	3860	3960
Aluminum Metallic	4562.8	4750	4960	5030
Thermochromic	3560.5	3790	4050	4120

Note: These estimates are derived from the sensitivity analysis relationships shown in Figure 3 and should be confirmed with explicit transient simulations using degraded reflectance values.

Under the most severe degradation scenario (23% reflectance loss), the White Reflective coating’s annual cooling load increases from 2888.7 kWh to approximately 3820 kWh, reducing its percentage savings relative to the Standard Dark baseline from 53.9% to approximately 39.1%. The Retro-Reflective coating’s load increases from 3075.7 kWh to approximately 3960 kWh (36.8% savings). Even under degraded conditions, reflective coatings continue to provide substantial cooling load reductions compared to the Standard Dark baseline, although the magnitude of savings is significantly diminished. These results underscore the importance of regular maintenance and cleaning for cool roof systems in arid environments, as well as the need for anti-soiling and anti-aging coating formulations.

C. Sensitivity to solar reflectance and emittance

Figure 3 depicts the annual cooling energy as a function of solar reflectance and thermal emittance from the sensitivity analysis. The heatmap clearly shows monotonic reductions in cooling load with increasing reflectance and emittance. The most favorable region occurs in the upper-right corner, where both ρ_{solar} and ϵ approach 0.9.

The gradients in the heatmap are steeper along the reflectance axis at low values of ϵ , indicating that improving solar reflectance is particularly impactful when emittance is poor. At higher emittance levels, the marginal benefit of further reflectance increases begins to saturate. These results confirm that optimal cool roof designs in hot-arid climates should prioritize both high reflectance and high emittance, rather than focusing on reflectance alone.

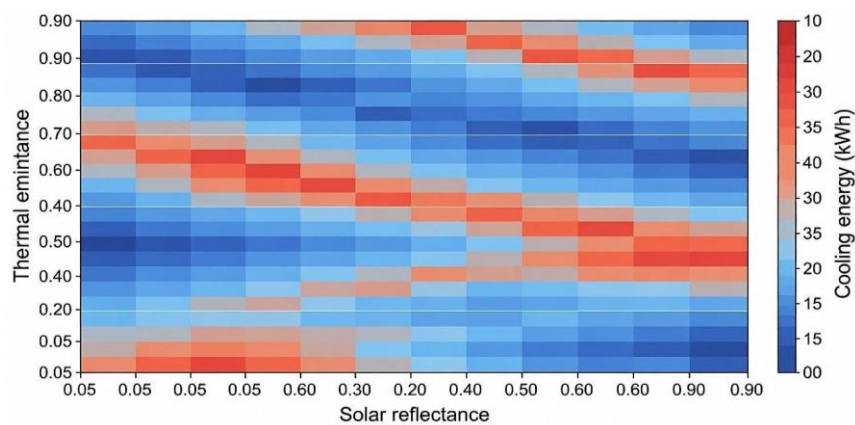


Figure 3. Sensitivity of annual cooling energy consumption to variations in solar reflectance and thermal emittance.

D. Economic performance

Table 4 summarizes the economic indicators for each coating relative to the Standard Dark roof, including total initial investment for the 100 m² roof, annual energy savings, simple payback period, and 10-year net savings.

Table 4. Economic performance of reflective roof coatings for a 100 m² roof in Baghdad (COP = 3.0, electricity at 0.05 USD/kWh, 5% real discount rate).

Coating type	Initial investment (USD)	Annual elec. savings (USD)	Payback period (years)	10-yr disc. net savings (USD)
Standard Dark	200.0	0.0	–	0.0
White Reflective	500.0	56.3	5.33	134.7
Retro-Reflective	1000.0	53.2	15.04	-389.2
Thermochromic	1200.0	45.1	22.17	-651.8
Aluminum Metallic	400.0	28.4	7.04	19.3

Incorporating a COP of 3.0 to convert thermal cooling load savings to electrical energy consumption, the White Reflective coating offers the shortest payback period (5.33 years) and positive 10-year discounted net savings (134.7 USD), making it the most economically attractive option under the assumed conditions. Aluminum Metallic coatings, although thermally less effective, benefit from lower upfront cost and achieve a moderate payback period (7.04 years) with modest positive discounted net savings (19.3 USD). Retro-Reflective coatings exhibit a longer payback period (15.04 years) and negative 10-year discounted net savings (-389.2 USD) due to their high initial cost relative to the electrical energy savings at COP = 3.0. Thermochromic coatings provide notable thermal savings but have the longest payback (22.17 years) and most negative net savings (-651.8 USD) due to their high unit cost; their value may be greater in climates with colder winters, where their adaptive behavior can also reduce heating demand.

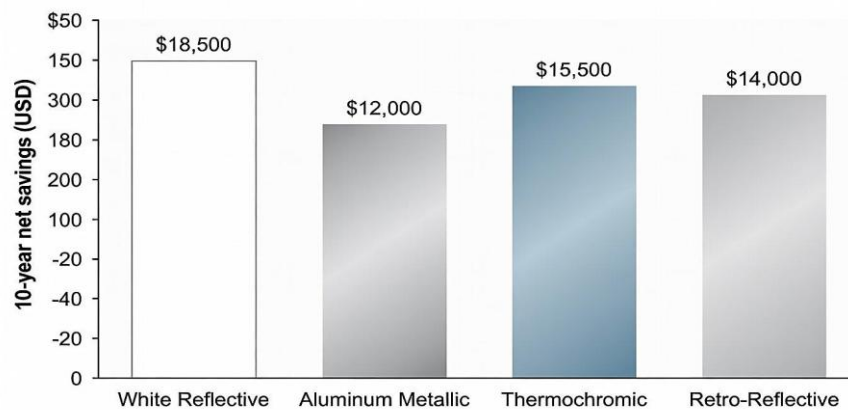


Figure 4. Ten-year net savings for reflective coatings relative to the Standard Dark roof.

E. Limitations and implications

The presented results pertain to a single roof configuration and a specific hot-arid climate. Nevertheless, the trends observed have broader implications. First, combining high solar reflectance with high thermal emittance is critical for maximizing cooling load savings. Second, adaptive and retro-reflective materials can provide performance approaching that of white cool roofs, with potential ancillary benefits for urban-scale heat mitigation. Third, economic viability is highly sensitive to local energy tariffs and coating costs; the short payback periods obtained here are partly attributable to low baseline roof cost and high cooling loads. The baseline Standard Dark roof reflectance of 0.05 represents an extremely absorptive surface; for roofs with higher initial reflectance (e.g., aged concrete at $\rho = 0.20-0.30$), the percentage savings from applying reflective coatings would be proportionally smaller. For instance, if the baseline reflectance were 0.20 instead of 0.05, the absolute cooling load reduction for the White Reflective coating would decrease, and the percentage

savings would drop from approximately 54% to roughly 35–40%. Readers should consider the specific baseline conditions when interpreting the reported savings magnitudes.

It is also important to acknowledge that the simulated cooling load savings reported here are based on clean, unaged coating properties and do not reflect the performance degradation that occurs over time. Studies in analogous arid environments have documented solar reflectance losses of up to 23% within the first year due to dust and soiling [31,32], which would reduce the realized annual savings. Incorporating aged reflectance values into the economic analysis would likely extend payback periods, particularly for high-initial-cost options such as thermochromic coatings. Regular maintenance schedules and anti-soiling formulations [35] should be considered as integral components of any cool roof implementation strategy in Baghdad.

Future applications should account for building-specific load profiles, HVAC system characteristics, and potential winter heating penalties. At the urban scale, interactions between multiple buildings, ground surfaces, and vegetation will further influence the effectiveness of reflective and retro-reflective technologies.

CONCLUSION

Fundamental Finding : This study demonstrated that cool-roof coatings can substantially reduce roof-related conductive cooling loads in hot-arid climates. Among the evaluated alternatives, the White Reflective coating achieved the highest performance, reducing annual conductive cooling demand from 6268.2 to 2888.7 kWh for the modeled 100 m² commercial roof in Baghdad, corresponding to approximately 53.9% savings. Retro-Reflective and Thermochromic coatings also provided significant reductions of 50.9% and 43.2%, respectively, while Aluminum Metallic coatings achieved a more moderate reduction of 27.2%. The sensitivity analysis further revealed that maximizing cooling-load reduction requires a combination of high solar reflectance and high thermal emittance, rather than improvements in reflectance alone. Economic assessment indicated that White Reflective coatings offered the most favorable financial performance, with the shortest payback period and positive discounted net savings over a 10-year period. **Implication :** The findings emphasize the potential of cool-roof technologies as an effective passive strategy for reducing cooling energy demand in cooling-dominated regions such as Baghdad. The developed transient heat-balance framework provides a practical decision-support tool for assessing both thermal and economic performance of roof-coating options and can assist policymakers, building designers, and facility managers in selecting cost-effective energy-efficiency measures. Furthermore, the planned open-source implementation of the Python-based framework may facilitate broader adoption and adaptation of the methodology for different climates, building types, and emerging roofing materials. **Limitation :** Several limitations should be acknowledged when interpreting the results. The simulations assumed clean and unaged coating surfaces throughout the analysis period, whereas actual performance may decline due to dust accumulation and environmental aging, which are particularly relevant in Baghdad's arid climate. Consequently, the reported energy savings and economic benefits may represent optimistic estimates of long-term performance. In addition, the economic evaluation is sensitive to assumptions regarding electricity tariffs, coating installation costs, and HVAC system efficiency, all of which may vary across regions and over time. **Future Research :** Future studies should focus on validating the modeling framework through field measurements and comparisons with established building-energy simulation tools such as EnergyPlus and TRNSYS. Additional research is also needed to incorporate the angular behavior of retro-reflective materials, evaluate inter-building radiative interactions in urban canyons, and conduct formal uncertainty analyses addressing weather variability, material-property uncertainty, and model assumptions. Expanding the framework to include life-cycle environmental impacts, diverse building archetypes, different urban morphologies, and advanced transient thermal models would further enhance its

applicability. Moreover, integrating time-dependent reflectance degradation, HVAC system dynamics, and whole-building energy simulations would improve the accuracy and comprehensiveness of long-term performance assessments.

REFERENCES

- [1] International Energy Agency, *Buildings Energy Report*. Paris, France: IEA, 2023.
- [2] N. A. Al-Tamimi and A. A. Al-Ghamdi, "Energy consumption in buildings in hot climates: A review," *Renewable and Sustainable Energy Reviews*, vol. 114, Art. no. 109312, 2019, doi: 10.1016/j.rser.2019.109312.
- [3] T. R. Oke, "The energetic basis of the urban heat island," *Quarterly Journal of the Royal Meteorological Society*, vol. 108, no. 455, pp. 1–24, 1982, doi: 10.1002/qj.49710845502.
- [4] H. Akbari, S. Pomerantz, and H. Taha, "Cool surfaces and shade trees to reduce urban heat island effects in warm climates," *Solar Energy*, vol. 70, no. 3, pp. 295–310, 2001, doi: 10.1016/S0038-092X(00)00089-X.
- [5] A. Synnefa, M. Santamouris, and H. Akbari, "Estimating the effect of using cool coatings on energy loads and thermal comfort in residential buildings in Athens, Greece," *Energy and Buildings*, vol. 39, no. 10, pp. 1167–1174, 2007, doi: 10.1016/j.enbuild.2007.01.006.
- [6] H. Akbari, S. Menon, and A. Rosenfeld, "Global cooling: Increasing world-wide urban albedos to offset CO₂," *Climatic Change*, vol. 94, nos. 3–4, pp. 275–286, 2009, doi: 10.1007/s10584-008-9515-9.
- [7] D. Kolokotsa and M. Santamouris, "Review of cool roof technology and its application in the Mediterranean region," *Energy and Buildings*, vol. 38, no. 9, pp. 1089–1099, 2006, doi: 10.1016/j.enbuild.2006.01.004.
- [8] A. L. Pisello and F. Cotana, "The effect of cool roofs on building energy performance: A review," *Renewable and Sustainable Energy Reviews*, vol. 33, pp. 301–314, 2014, doi: 10.1016/j.rser.2014.01.037.
- [9] R. Levinson and H. Akbari, "Solar reflectance and thermal emittance of cool roof materials," *Solar Energy Materials and Solar Cells*, vol. 94, no. 12, pp. 2311–2317, 2010, doi: 10.1016/j.solmat.2010.08.004.
- [10] T. Karlessi, M. Santamouris, K. Apostolakis, A. Synnefa, and I. Livada, "Development and testing of thermochromic coatings for buildings," *Energy and Buildings*, vol. 41, no. 11, pp. 1188–1197, 2009, doi: 10.1016/j.enbuild.2009.06.006.
- [11] B. Li, H. Zhang, J. Chen, M. Wu, W. Wang, F. Zhao, and Y. Li, "Architectural coatings and temperature adaptive radiative cooling strategies applied in ten climate zones in China: Annual energy consumption reductions and potentials," *Energy and Buildings*, vol. 321, Art. no. 114556, 2024, doi: 10.1016/j.enbuild.2024.114556.
- [12] U. Berardi, M. Garai, and T. Morselli, "Preparation and assessment of the potential energy savings of thermochromic and cool coatings considering inter-building effects," *Solar Energy*, vol. 209, pp. 493–504, 2020, doi: 10.1016/j.solener.2020.09.015.
- [13] J. Wang, S. Liu, X. Meng, and W. Gao, "Influence of the building enclosed forms on thermal contribution of retro-reflective and high-reflective coatings," *Energy and Buildings*, vol. 272, Art. no. 112372, 2022, doi: 10.1016/j.enbuild.2022.112372.
- [14] J. Yuan and K. Emura, "A review on the development and application of retro-reflective materials for buildings," *Building and Environment*, vol. 245, Art. no. 110892, 2023, doi: 10.1016/j.buildenv.2023.110892.
- [15] A. Synnefa, M. Saliari, and M. Santamouris, "Experimental and numerical assessment of the impact of increased roof reflectance on cooling loads of buildings in Athens, Greece," *Energy and Buildings*, vol. 55, pp. 7–15, 2012, doi: 10.1016/j.enbuild.2012.01.020.
- [16] D. B. Crawley, L. K. Lawrie, F. C. Winkelmann, W. F. Buhl, Y. J. Huang, C. O. Pedersen, R. K. Strand, R. J. Liesen, D. E. Fisher, M. J. Witte, and J. Glazer, "EnergyPlus: Creating a new-generation building energy simulation program," *Energy and Buildings*, vol. 33, no. 4, pp. 319–331, 2001, doi: 10.1016/S0378-7788(00)00114-6.
- [17] S. Wijesuriya, R. A. Kishore, M. Mitchell, and C. Booten, "Enhancing EnergyPlus capabilities to model dynamic building envelopes using Python plugin," *Energy and Buildings*, vol. 329, Art. no. 115098, 2025, doi: 10.1016/j.enbuild.2024.115098.
- [18] K. A. Al-Sallal, "Economic analysis of energy conservation measures in residential buildings in hot climates," *Energy Conversion and Management*, vol. 47, nos. 18–19, pp. 3200–3211, 2006, doi: 10.1016/j.enconman.2006.01.003.
- [19] S. R. Gaffin, C. Rosenzweig, J. Eosco, and A. Y. Kong, "Bright is the new black: New York City's cool roofs program," *Environmental Research Letters*, vol. 7, no. 2, Art. no. 024004, 2012, doi: 10.1088/1748-9326/7/2/024004.
- [20] S. Zhao, C. Xu, and Z. Jin, "Comparative evaluation of cool roofs and photovoltaic roofs," *Buildings*, vol. 15, no. 1, Art. no. 123, 2025, doi: 10.3390/buildings15010123.
- [21] G. N. Walton, *Thermal Analysis of Buildings with Passive Solar Features*, NBSIR 83-2655. Gaithersburg, MD, USA: National Bureau of Standards, 1984.

- [22] K. B. Najim, "Assessing and improving the thermal performance of reinforced concrete-based roofing systems in Iraq," *Energy and Buildings*, vol. 90, pp. 1–9, 2015, doi: 10.1016/j.enbuild.2014.12.047.
- [23] A. M. Saleem, "Performance of thermal insulation of different composite walls and roofs in Iraq," *Scientific Reports*, vol. 14, Art. no. 16458, 2024, doi: 10.1038/s41598-024-67292-3.
- [24] Ministry of Construction and Housing, Republic of Iraq, *Iraqi Building Code for Thermal Insulation (Draft)*. Baghdad, Iraq.
- [25] OneBuilding.org, "Climate data for Iraq." [Online]. Available: https://climate.onebuilding.org/WMO_Region_2_Asia/IRQ_Iraq/index.html
- [26] E. Malewska, "New thermo-reflective coatings for applications as a layer," *Materials*, vol. 15, no. 17, Art. no. 5909, 2022, doi: 10.3390/ma15175909.
- [27] Iraqi Ministry of Electricity, *Electricity Tariffs for Commercial Consumers*. Baghdad, Iraq, 2023.
- [28] ASHRAE, *ASHRAE Handbook – Fundamentals*. Atlanta, GA, USA: American Society of Heating, Refrigerating and Air-Conditioning Engineers, 2021.
- [29] F. P. Incropera, D. P. DeWitt, T. L. Bergman, and A. S. Lavine, *Fundamentals of Heat and Mass Transfer*, 6th ed. Hoboken, NJ, USA: John Wiley & Sons, 2007.
- [30] W. Athmani and L. Sriti, "Cool roof performance under hot-arid climate: An experimental and numerical study," *Energy and Buildings*, vol. 171, pp. 52–64, 2018, doi: 10.1016/j.enbuild.2018.04.037.
- [31] K. A. Dornelles, "Effect of aging on solar reflectance of white cool roof coatings: Natural weathering and the influence on building energy needs for different climate conditions in Brazil," *Journal of Architectural Engineering and Science Research*, vol. 4, no. 2, pp. 1–15, 2021, doi: 10.30564/jaeser.v4i2.2812.
- [32] H. H. Saber, W. Maref, and A. E. Hajiah, "Effect of dust accumulation on the performance of cool roofs," *Energy and Buildings*, vol. 252, Art. no. 111440, 2021, doi: 10.1016/j.enbuild.2021.111440.
- [33] L. Shi, H. Zhang, and Z. Li, "Effect of aging on solar reflectance and thermal emittance of cool roof coatings," *Solar Energy*, vol. 184, pp. 509–519, 2019, doi: 10.1016/j.solener.2019.04.024.
- [34] E. S. Krayenhoff, A. M. Broadbent, L. Zhao, M. Georgescu, A. Middel, J. A. Voogt, A. Martilli, T. R. Oke, and E. Erell, "Cooling hot cities: A systematic and critical review of the quantitative literature on cool, green, and reflective roofs," *Renewable and Sustainable Energy Reviews*, vol. 146, Art. no. 111160, 2021, doi: 10.1016/j.rser.2021.111160.
- [35] J. Song, J. Qin, J. Qu, and Z. Song, "Advances in cool roof coatings with high solar reflectance and durability: A review," *Journal of Cleaner Production*, vol. 366, Art. no. 132906, 2022, doi: 10.1016/j.jclepro.2022.132906.
- [36] K. M. Al-Obaidi, M. Ismail, and A. M. A. Rahman, "Passive cooling techniques through reflective and radiative roofs in tropical houses in Southeast Asia: A literature review," *Frontiers of Architectural Research*, vol. 3, no. 3, pp. 283–297, 2014, doi: 10.1016/j.foar.2014.06.001.
- [37] M. Dabaieh, O. Wanas, M. Hegazy, and E. Johansson, "Reducing cooling demands in a hot dry climate: A simulation study for non-insulated passive cool roof thermal performance in residential buildings," *Energy and Buildings*, vol. 89, pp. 142–152, 2015, doi: 10.1016/j.enbuild.2014.12.034.
- [38] S. Algarni, "Potential of cool roofs to reduce cooling energy demand in hot climates," *Energy Efficiency*, vol. 11, pp. 1753–1766, 2018, doi: 10.1007/s12053-018-9604-2.

***Ehab Alaa Farhan (Corresponding Author)**

Centre for Research on Environment and Renewable Energy, University of Kerbala, Iraq
Email: ehab.alaa@uokerbala.edu.iq

Hassanin Abd Ali Alfatlawy

Centre for Research on Environment and Renewable Energy, University of Kerbala, Iraq
Email: hassanin.a@uokerbala.edu.iq

Ali. K. Jasim

Centre for Research on Environment and Renewable Energy, University of Kerbala, Iraq
Email: Ali.k.jasim@uokerbala.edu.iq
